Comparative Biochemistry and Physiology, Part B 155 (2010) 230–240

Contents lists available at ScienceDirect

Comparative Biochemistry and Physiology, Part B

journal homepage: www.elsevier.com/locate/cbpb

NTPDase family in zebrafish: Nucleotide hydrolysis, molecular identification and gene expression profiles in brain, liver and heart

Denis Broock Rosemberg [a,b], Eduardo Pacheco Rico [a,b], Andrei Silveira Langoni [c], Jonathan Tesch Spinelli [c], Talita Carneiro Pereira [d], Renato Dutra Dias [c], Diogo Onofre Souza [a,b], Carla Denise Bonan [c,e,*], Maurício Reis Bogo [d,e,*]

[a] Programa de Pós-graduação em Bioquímica, Departamento de Bioquímica, Instituto de Ciências Básicas da Saúde, Universidade Federal do Rio Grande do Sul. Rua Ramiro Barcelos 2600-Anexo, 90035-003, Porto Alegre, RS, Brazil
[b] Instituto Nacional em Excitotoxicidade e Neuroproteção (INCT-EN) 90035-003, Porto Alegre, RS, Brazil
[c] Laboratório de Neuroquímica e Psicofarmacologia, Departamento de Biologia Celular e Molecular, Faculdade de Biociências, Pontifícia Universidade Católica do Rio Grande do Sul. Avenida Ipiranga, 6681, 90619-900, Porto Alegre, RS, Brazil
[d] Laboratório de Biologia Genômica e Molecular, Departamento de Biologia Celular e Molecular, Faculdade de Biociências, Pontifícia Universidade Católica do Rio Grande do Sul. Avenida Ipiranga, 6681, 90619-900, Porto Alegre, RS, Brazil
[e] Instituto Nacional Translacional em Medicina (INCT-TM), 90035-003, Porto Alegre, RS, Brazil

ARTICLE INFO

Article history:
Received 25 September 2009
Received in revised form 9 November 2009
Accepted 9 November 2009
Available online 14 November 2009

Keywords:
NTPDase
Zebrafish
Nucleotide hydrolysis
Phylogenetic analysis
Gene expression profiles

ABSTRACT

The nucleoside triphosphate diphosphohydrolase (NTPDase) family cleaves tri- and diphosphonucleosides to monophosphonucleosides and is responsible for terminating purinergic transmission. Since the NTPDase family in zebrafish is poorly understood, here we evaluated the nucleotide hydrolysis in three tissues of adult zebrafish (brain, liver, and heart), confirmed the presence of distinct NTPDase members by a phylogenetic analysis and verified their relative gene expression profiles in the respective tissues. A different profile of ATP and ADP hydrolysis in the brain, liver, and heart as a function of time and protein concentration was observed. Sodium azide (20 mM), ARL 67156 (300 μM) and Suramin (300 μM) differently altered the nucleotide hydrolysis in zebrafish tissues, suggesting the contribution of distinct NTPDase activities. Homology-based searches identified the presence of NTPDase1-6 and NTPDase8 orthologs and the phylogeny also grouped three NTPDase2 and two NTPDase5 paralogs. The deduced amino acid sequences share the apyrase conserved regions, conserved cysteine residues, putative *N*-glycosylation, phosphorylation, N-acetylation sites, and different numbers of transmembrane domains. RT-PCR experiments revealed the existence of a distinct relative *entpd1-6* and *entpd8* expression profile in brain, liver, and heart. Taken together, these results indicate that several NTPDase members might contribute to a tight regulation of nucleotide hydrolysis in zebrafish tissues.

1. Introduction

The NTPDase family consists of enzymes that hydrolyze tri- and diphosphonucleosides into their monophosphate counterparts and thus plays a crucial role in nucleotide catabolism. After release into the synaptic cleft ATP and other nucleotides undergo rapid enzymatic degradation by ectonucleotidases, which are functionally important because ATP metabolites act as physiological ligands for various purinergic receptors (Burnstock, 2009). In this sense, NTPDase activities not only control the lifetime of nucleotides but, by degrading or interconverting the originally released ligands, they also produce ligands for additional P2 receptors and nucleosides (Zimmermann, 2006). Common features that characterize NTPDase family members are the presence of five apyrase conserved regions (ACRs) and the requirement for divalent cations for enzyme activity (Zimmermann, 2001; Kirley et al., 2006). The eight NTPDase members hydrolyze their substrates with distinct ability and specificity and differ according to their cellular location (Zimmermann, 2001). For example, NTPDases1–3 and 8 are expressed as cell surface-located enzymes being anchored to the plasma membrane via two transmembrane domains, whereas NTPDases4–7 face the lumen of cytoplasmic organelles (Lavoie et al., 2004). While NTPDases4 and 7 contain two transmembrane domains that are entirely intracellular, NTPDases5 and 6 have a single transmembrane domain and undergo secretion after heterologous expression (Murphy-Piedmonte et al., 2005).

The importance of nucleotide hydrolysis for homeostasis in several tissues has been extensively reported. Changes in neuronal plasticity, inhibitory avoidance learning, seizure activity, and cerebral ischemia have been correlated with alterations in NTPDase activities (Bonan

* Corresponding authors. Instituto Nacional Translacional em Medicina (INCT-TM), 90035-003, Porto Alegre, RS, Brazil. Tel.: +55 51 3320 3500x4726 / 4158; fax: +55 51 3320 3568.
E-mail addresses: cbonan@pucrs.br (C.D. Bonan), mbogo@pucrs.br (M.R. Bogo).

1096-4959/$ – see front matter © 2009 Elsevier Inc. All rights reserved.
doi:10.1016/j.cbpb.2009.11.005

et al., 1998, 2000; Schetinger et al., 2007). It has been shown that NTPDase1 activity coordinates both hepatocyte and endothelial cell proliferation in mouse liver, suggesting that purines are involved in hepatic regeneration and vascular reconstitution (Beldi et al., 2008). Furthermore, NTPDase1 also promotes myocardial protection during cardiac ischemia/reperfusion injury (Köhler et al., 2007) and its activity and expression profile have been characterized in rat heart ventricle (Rücker et al., 2008). The prevention of excessive contractility in cardiomyocytes has been attributed to *entpd3* expression, giving support to the suggestion that distinct NTPDase members act in a coordinated manner to maintain heart homeostasis (Barreto-Chaves et al., 2006).

Zebrafish (*Danio rerio*) have been used as an animal model for biomedical research of numerous pathologies, such as seizures (Baraban, 2007), liver failure (Rekha et al., 2008), and cardiac malfunctions (Chico et al., 2008). The P2X receptor gene family and the nucleotide hydrolysis in brain membranes have already been characterized in zebrafish (Kucenas et al., 2003; Rico et al., 2003; Senger et al., 2004). In addition, the expression of *entpd1*, three *entpd2*, and *entpd3* genes (Rico et al., 2006; Appelbaum et al., 2007) and the immunocytochemical localization of NTPDase1 and 2 in the neural retina of zebrafish (Ricatti et al., 2009) suggest the existence of a compartmentalized regulation of extracellular nucleotide/nucleoside concentration in this teleost.

Since the investigation of NTPDase family members in complementary vertebrate models is relevant to better understand this enzyme group, the study of the NTPDases in zebrafish is imperative and raises the perspective of performing structural and functional comparisons of distinct purinergic signaling parameters between fish and mammals. Although recent studies demonstrated the existence of NTPDase activities in zebrafish (Rico et al., 2006; Ricatti et al., 2009), the identification of cell surface-located and intracellular NTPDase members which might contribute to ATP and ADP hydrolysis in different tissues and the detection of their mRNAs have not yet been reported.

Here we assay the nucleotide hydrolysis and test the influence of distinct inhibitors of ATP and ADP hydrolysis in zebrafish brain, liver, and heart. To specifically verify whether different NTPDase members could be involved in nucleotide catabolism in these respective tissues, we used homology-based searches and a phylogenetic analysis to identify the zebrafish NTPDase sequences. Furthermore, we also evaluated some special features of the deduced amino acid sequence obtained using bioinformatics tools and analyzed the gene expression profile of the *entpd* members in these tissues.

2. Materials and methods

2.1. Animals

Adult males and females of the "wild type" (short fin — SF) zebrafish (*Danio rerio*) strain (3–6 months-old, weighing 0.32 ± 0.06 g) were obtained from a commercial distributor (Delphis, RS, Brazil) and acclimated for at least 2 weeks before the experiments. The animals were maintained in a 50-L thermostated aquarium filled with continuously aerated unchlorinated water at a targeted temperature of 26 ± 2 ºC under a 12-h light-dark photoperiod, and fed twice a day to satiety with commercial flake fish food. Before the experiments, the fish were cryoanaesthetized and euthanized by decapitation. Each independent experiment was performed using biological preparations from five different animals. The animals were raised and cared for according to the National Institute of Health Guide for Care and Use of Laboratory Animals.

2.2. Chemicals

Trizma Base, ammonium molybdate, polyvinyl alcohol, Malachite Green, nucleotides, EDTA, EGTA, sodium citrate, Coomassie Blue G, bovine serum albumin, calcium chloride, ouabain, Ap5A, NEM, orthovanadate, levamisole, oligomycin, sodium azide, ARL 67156 (6-N,N-diethyl-D-β,γ-dibromomethylene adenosine triphosphate) and Suramin were purchased from Sigma Aldrich (St. Louis, MO, USA). TRIzol, SuperScript™ III First-Strand Synthesis SuperMix, Taq Platinum, GelRed and Low DNA Mass Ladder were purchased from Invitrogen (Carlsbad, CA, USA). All other reagents used were of high analytical grade.

2.3. Nucleotide hydrolysis assay

Tissues (brain, liver, and heart) were dissected and added to 1 mL of chilled Tris–citrate buffer (50 mM Tris–citrate, 2 mM EDTA, 2 mM EGTA, pH 7.4, adjusted with citric acid) as described by Barnes et al. (1993). This same buffer has been also used in previous studies (Rico et al., 2003; Senger et al, 2004) to exclude a possible interference of endogenous divalent cations (such as Ca^{2+} and Mg^{2+}) during tissue preparation, which could influence the nucleotidase activities assayed. The samples were homogenized on ice in a motor-driven Teflon-glass homogenizer and centrifuged at 1000 *g* for 10 min at 4 °C to remove the nuclei and cell debris. The resultant supernatants were kept on ice and used for the enzyme assays.

The optimum conditions for ATP and ADP hydrolysis were determined for each tissue. Brain, liver, and heart samples (3–5 μg protein) were added to the reaction mixture containing 50 mM Tris–HCl (pH 8.0) and 5 mM $CaCl_2$ in a final volume of 200 μL. The samples were preincubated for 10 min at 37 °C before starting the reaction with the addition of substrate (ATP or ADP) every 10 s to a final concentration of 1 mM. After incubation for 20 min (brain and liver) and 30 min (heart), the reactions were terminated with the addition of 200 μL of 10% trichloroacetic acid every 10 s for each sample to ensure the correct incubation time and immediately placed on ice for 10 min. Controls with the addition of the enzyme preparation after mixing with trichloroacetic acid were used to correct non-enzymatic hydrolysis of substrates. The inorganic phosphate (Pi) released was measured spectrophotometrically at 630 nm using Malachite Green solution as color reagent (Chan et al., 1986) and KH_2PO_4 as standard after 4-fold dilution to ensure that the concentration of phosphate was within the linear range. Incubation times and protein concentrations were chosen in order to ensure the linearity of the reactions. All enzyme assays were run in triplicate and the specific activity was expressed as nmol Pi min^{-1} mg $protein^{-1}$.

2.4. Protein measurement

Protein concentration for the enzyme assays was measured by the Coomassie blue method (Bradford, 1976), with bovine serum albumin as standard.

2.5. In silico confirmation of zebrafish NTPDase sequences

The well-known human and mouse NTPDase protein sequences were used as queries (Table 1) to perform a Basic Local Alignment Search (BLASTP function) via the GenBank, ENSEMBL, and ZFIN *Danio rerio* databases. The NTPDase protein sequences obtained were aligned through the ClustalX program (Thompson et al., 1997) and analyzed using bioinformatics tools available at CBS Prediction Servers (http://www.cbs.dtu.dk/services/). A phylogenetic tree was built with the MEGA 4.0 program (Tamura et al., 2007) and the statistical Neighbor-Joining method (Saitou and Nei, 1987) with proportional (*p*) distance was used. The percent identity and similarity between the zebrafish and mammalian NTPDase proteins were determined by the scoring matrix BLOSUM62 using MatGAT 2.01 software (Campanella et al., 2003). All NTPDase sequences identified are presented in Table 2.

Table 1
Mammalian NTPDase orthologs used in phylogenetic analysis.

Species	GenBank acession number
Human (*Homo sapiens*)	
NTPDase1	NP_001767
NTPDase2	NP_982293
NTPDase3	NM_001248
NTPDase4	BC034477
NTPDase5	NM_001249
NTPDase6	BC025980
NTPDase7	NM_020354
NTPDase8	AAR04374
Mouse (*Mus musculus*)	
NTPDase1	AAH11278
NTPDase2	O55026
NTPDase3	AY376710
NTPDase4	BC043134
NTPDase5	BC015247
NTPDase6	BAE33807
NTPDase7	NM_053103
NTPDase8	AAQ84519

2.6. Primer design and RT-PCR experiments

The *entpd1*, *entpd2_mg*, *entpd2_mq*, and *entpd2_mv* primers were designed as described previously (Rico et al., 2006). Zebrafish DNA sequences encoding each of the NTPDase members retrieved from the GenBank database were aligned using the ClustalX program. Regions with low scores for similarity among the sequences were used to search for specific primers, which were designed using the program Oligos 9.6. The primer specificities were checked by comparing each primer with the zebrafish genome to confirm that it would recognize only its specific target sequence. Thus, the strategy adopted to design the primers avoided cross-amplification. The *β-actin* primers employed were previously described by Chen et al. (2004) and the optimal PCR conditions for *entpd* amplifications were determined (Table 3).

Brain, liver, and heart were dissected under sterile conditions and immediately subjected to a total RNA extraction by the TRIzol method according to the manufacturer's instructions. The purity of the RNA was spectrophotometrically quantified by calculating the ratio between absorbance values at 260 and 280 nm and its integrity was confirmed by electrophoresis through a 1.0% agarose gel. Afterwards, all samples were adjusted to 160 ng/μL and cDNA species were synthesized using SuperScript™ III First-Strand Synthesis SuperMix.

PCR conditions were optimized in order to determine the number of cycles that would allow product detection within the linear phase of band intensities analyzed. The reactions were performed in a final volume of 20 μL, using 0.1 μM primers (Table 2), 0.2 μM dNTP, 2 mM $MgCl_2$ and 0.5 U Taq Platinum for *β-actin* amplification. The same conditions were employed for the *entpd2_mg*, *entpd2_mq*, *entpd2_mv*, *entpd3*, *entpd4*, *entpd5_me*, and *entpd6* genes, with the addition of 1 M betain for PCR experiments on the three *entpd2* genes. The *entpd1* and *entpd5_ms* reactions were performed using 3 mM $MgCl_2$ and 1 M betain was also employed for *entpd1* amplification. PCR assays for the *entpd8* gene were carried out using 2.5 mM $MgCl_2$, 0.2 μM dNTP and 1 U Taq Platinum. All PCR experiments were performed using 1 μL of template cDNA.

The following conditions were used for PCR reactions: 1 min at 94 °C, 1 min at the annealing temperature (see Table 3), 1 min at 72 °C for 30 cycles (for *entpd3*, *entpd4*, *entpd5_me*, and *entpd6*) and for 35 cycles (for *β-actin*, *entpd1*, *entpd2_mg*, *entpd2_mq*, *entpd2_mv*, *entpd5_ms*, and *entpd8*) with a further post-extension cycle at 72 °C

Table 3
Primer characteristics for *entpd* and *β-actin* genes.

Gene	Primer sequences (5′-3′)	Annealing	PCR fragment (bp)
entpd1	CCCATGGCACAGGCCGGTTG (forward) GCAGTCTCATGCCAGCCGTG (reverse)	54	380
*entpd2_mg**	GGAAGTGTTTGACTCGCCTTGCACG (forward) CAGGACACAAGCCCTTCCGGATC (reverse)	62	554
*entpd2_mq**	CCAGCGGATTTAGAGCACGCTG (forward) GAAGAACGGCGGCACGCCAC (reverse)	62	313
*entpd2_mv**	GCTCATTTAGAGGACGCTGCTCGTG (forward) GCAACGTTTTCGGCAGGCAGC (reverse)	62	263
entpd3	TACTTTCTTTGGACAGAGCAACCCTG (forward) AAGCATATAGCCCAGGGACCAGG (reverse)	62	424
entpd4	CGTGGTTCTGGAGACTTTGAGCGCTG (forward) TGTCCTGAGGTTCTCATACGCCGCTG (reverse)	60	387
*entpd5_ms**	CCGCCAGGTCAACTTCAGTCGCGTC (forward) TCTTTGACCTCATTCAGCAGGGCTTTG (reverse)	57	333
*entpd5_me**	TTCTGCTGCTGCTGATTTCTCGGTGC (forward) ATGATCCTGACGCTGTCTGGAGGAACG (reverse)	60	438
entpd6	TGAAGGCCAGCCTTTAGCGGGAC (forward) CCTGTGCGTTCATCAATGAGGCCCAG (reverse)	60	270
entpd8	AGCTTTATTAAGCACACATTTGAGGGCTC (forward) GGGGTTGAAACTGCTTGGTGGGACC (reverse)	58	363
*β-actin***	GTCCCTGTACGCCTCTGGTCG (forward) GCCGGACTCATCGTACTCCTG (reverse)	54	678

*Corresponds to the first two amino acid residues of the protein sequence.
**PCR primer sequences previously described (Chen et al., 2004).

Table 2
Identified members of the NTPDase family in zebrafish.

Gene	Protein	Chromosome	Amino acid residues	ENSEMBL	Accession numbers	
					GenBank	ZFIN ID
entpd1	NTPDase1	12	492	ENSDARP00000066256	AAH78240	ZDB-GENE-040801-58
entpd2_mg [a]	NTPDase2_mg	21	509	Not identified	XP_697600	Not identified
entpd2_mq [a]	NTPDase2_mq	5	497	ENSDARP00000043258	XP_687722	ZDB-GENE-040724-67
entpd2_mv [a]	NTPDase2_mv	5	502	ENSDARP00000051433	AAH78419	ZDB-GENE-040724-187
entpd3	NTPDase3	16	518	ENSDARP00000094926	ABR15509	ZDB-GENE-030131-6186
entpd4	NTPDase4	8	611	ENSDARP00000056073	NP_001002419	ZDB-GENE-040718-116
entpd5_ms [a]	NTPDase5_ms	17	450	Not identified	XP_684862	Not identified
entpd5_me [a]	NTPDase5_me	25	525	Not identified	XP_001339099	Not identified
entpd6	NTPDase6	17	442	ENSDARP00000037620	NP_001017862	ZDB-GENE-050417-412
entpd8	NTPDase8	6	484	ENSDARP00000008913	NP_001002379	ZDB-GENE-040724-142

[a] Correspond to the first two amino acid residues from protein sequences.

for 10 min. A negative control was included for each set of PCR reactions. PCR products were separated on a 1.0% agarose gel with GelRed 10× and visualized with ultraviolet light. The fragment lengths expected for the PCR reactions were confirmed using Low DNA Mass Ladder and *β-actin* was determined as an internal standard. Band intensities were analyzed by optical densitometry using the software ImageJ 1.37 for Windows after running all PCR products in a single gel.

2.7. Statistical analysis

All assays were performed in triplicate and means ± S.E.M. of at least three independent experiments were presented. Data were analyzed by one-way analysis of variance (ANOVA). Post-hoc comparisons were made using Tukey's HSD test (for gene expression data) or Dunnett's Multiple Comparison Test (for the experiments with inhibitors) and differences were considered statistically significant at a $P \leq 0.05$ level.

3. Results

3.1. Nucleotide hydrolysis in zebrafish tissues

The ability of different zebrafish tissues to hydrolyze both ATP and ADP was tested as a function of time and protein concentration in order to determine the correct assay conditions (Fig. 1). The incubation with the respective nucleotides (1 mM) showed that the time courses for ATP and ADP hydrolysis were linear up to 40 min for the brain and liver (Fig. 1A and B) and up to 60 min for the heart (Fig. 1C). Furthermore, nucleotide hydrolysis increased as a function of protein concentration and product formation was linear in the range of 3–10 μg protein in the incubation medium for the brain and liver (Fig. 1D and E) and 3–5 μg protein for the heart (Fig. 1F). Concerning nucleotide preference, further experiments using 3–5 μg protein and an incubation time of 20 min (brain and liver) and 30 min (heart) demonstrated that ADP hydrolysis was significantly lower than ATP hydrolysis in the brain (36%) and heart (49%), whereas no significant difference was found in the liver (data not shown).

The correlation between NTPDase activities with ATPases and alkaline phosphatase was also evaluated. The classical inhibitors of Na^+- K^+-ATPase (ouabain and orthovanadate), Ca^{2+}, Mg^{2+}-ATPase (NEM), alkaline phosphatase (levamisole), and adenylate kinase (P^1, P^5-di (adenosine 5′-)pentaphosphate, Ap_5A) did not induce significant changes in nucleotide hydrolysis in zebrafish tissues (data not shown). However, some compounds associated with an inhibitory effect on NTPDase activities did alter the nucleotide hydrolysis in brain (Fig. 2A), liver (Fig. 2B) and heart (Fig. 2C). Sodium azide (20 mM), which has been considered an inhibitor of ATP diphosphohydrolase from several sources, significantly inhibited ATP and ADP hydrolysis in brain (34% and 63%, respectively), liver (34% and 30%, respectively), and heart (45% and 40%,

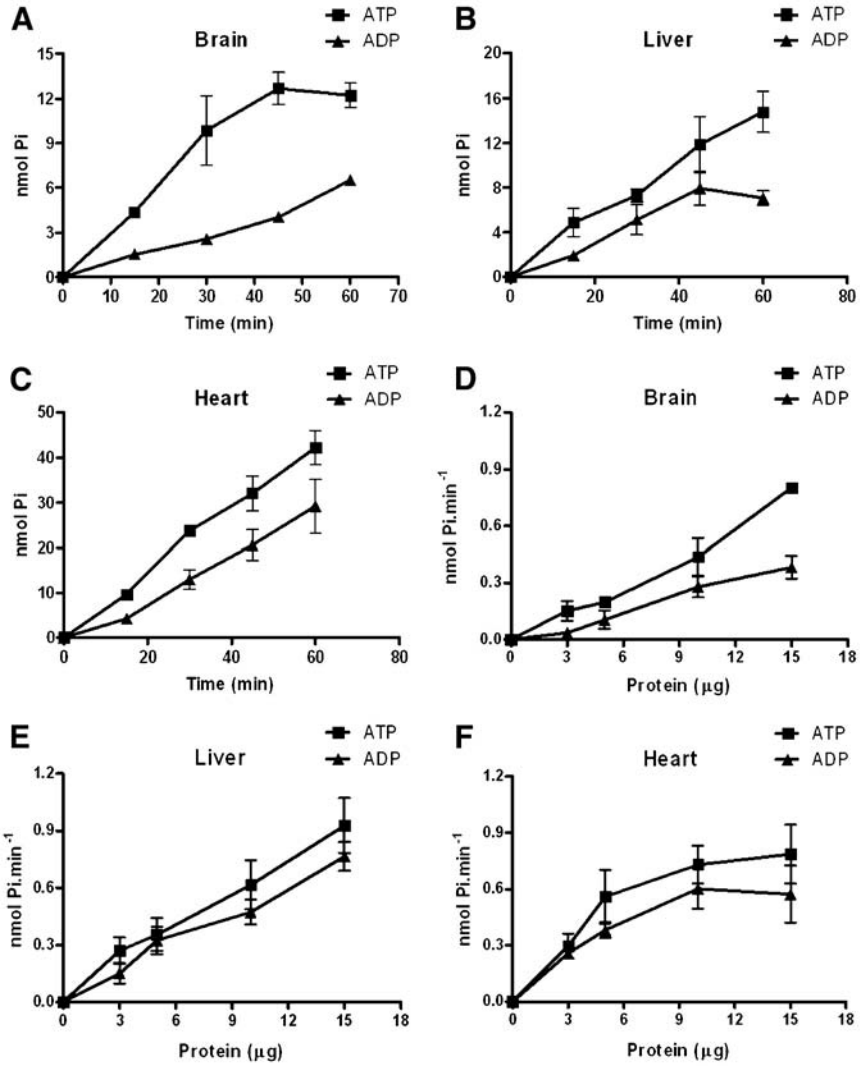

Fig. 1. Time courses (A–C) for Ca^{2+}-ATP and Ca^{2+}-ADP hydrolysis in 3–5 μg fractions of zebrafish brain (A), liver (B), and heart (C). Effect of different protein concentrations (D–F) on Ca^{2+}-ATP and Ca^{2+}-ADP hydrolysis in zebrafish brain (D), liver (E), and heart (F). Data represent means ± S.E.M of four different experiments, each in duplicate.

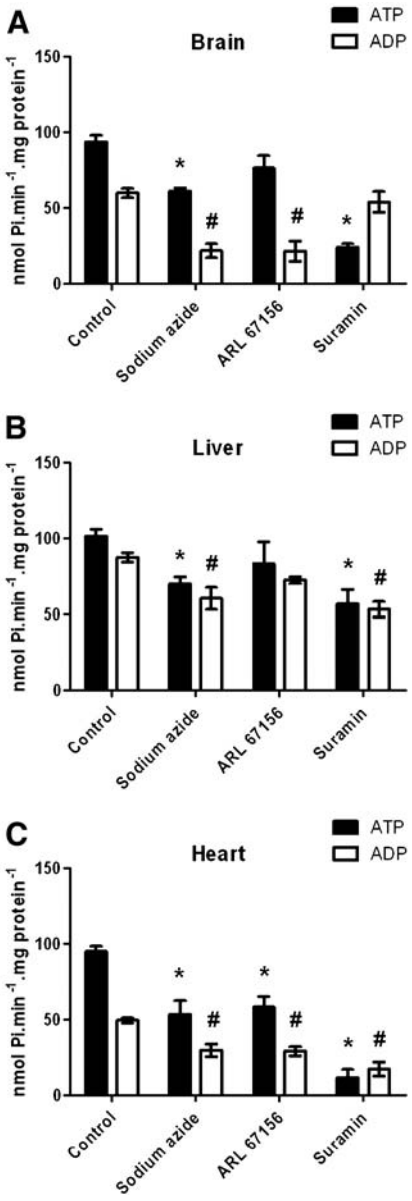

Fig. 2. Effect of putative NTPDase inhibitors (sodium azide 20 mM, ARL 67156 300 μM and Suramin 300 μM) on ATP (black bars) and ADP (white bars) hydrolysis in the brain (A), liver (A), and heart (C) of zebrafish. Data represent the means ± S.E.M of three different experiments. The asterisks (*) represent significant differences in ATP hydrolysis when compared to control and the symbol (#) represents significant differences in ADP hydrolysis when compared to control (ANOVA, followed by Dunnett's Multiple Comparison Test as post-hoc, $P \leq 0.05$).

respectively). Moreover, treatment with two ATPDase inhibitors (300 μM ARL 67156 and 300 μM Suramin) differentially altered the nucleotide hydrolysis. ARL 67156 inhibited ADP hydrolysis in brain (18%) and also caused a significant decrease in ATP (39%) and ADP (41%) hydrolysis in heart. Suramin strongly inhibited ATP hydrolysis in the brain (74%) and hydrolysis of both nucleotides in the heart (88% and 65% for ATP and ADP, respectively). A weaker inhibitory effect was observed for Suramin against ATP and ADP hydrolysis in liver (44% and 39%, respectively). These results strongly suggest the presence of different NTPDase activities in the brain, liver, and heart of zebrafish.

3.2. Phylogenetic analysis of zebrafish NTPDase family

Considering that ATP and ADP hydrolysis in different tissues involves the contribution of several enzyme activities, the presence of distinct zebrafish NTPDase family members was investigated. The well-known *Homo sapiens* and *Mus musculus* NTPDase proteins were used as queries to obtain the zebrafish NTPDase orthologs. Searches in GenBank, ENSEMBL, and ZFIN databases lead to the identification of ten putative NTPDase sequences (Table 2). The phylogeny constructed resulted in eight well-resolved terminal clades confirming the presence of ten NTPDase orthologs for zebrafish. The graphic depiction of a multiple sequence alignment of zebrafish and mammalian members of the NTPDase family illustrates the subdivision of the family into surface-located and intracellular enzymes (Fig. 3). Among all identified sequences, five members (NTPDase1, three NTPDase2 paralogs, and NTPDase3) had been previously shown to exist (Rico et al., 2006; Appelbaum et al., 2007). However, two NTPDase5 paralogs (NTPDase5_ms and NTPDase5_me), NTPDase6, and NTPDase8 orthologs were identified by phylogenetic analysis for the first time. The putative NTPDase8 sequence was obtained only when mammalian orthologs were compared to the zebrafish protein database at ENSEMBL. The searches performed did not allow the identification of a zebrafish NTPDase7 sequence.

3.3. Properties of the NTPDase members in zebrafish

The chromosome location, accession numbers (GenBank, ENSEMBL, and ZFIN), and number of amino acid residues of the distinct zebrafish NTPDase members are presented in Table 2. In order to compare the zebrafish proteins with their mammalian orthologs, the deduced amino acid sequences were aligned and the percent identity and similarity were determined.

The relatedness between the surface-located and intracellular NTPDase members is shown in Table 4A and 4B, respectively. Zebrafish sequences generally have a percent identity of around 50% when compared to mouse and human NTPDase orthologs. Nevertheless, NTPDase4 exhibits a percent identity of around 70% when compared to the respective mouse and human orthologs. The high percent identity and similarity among vertebrate NTPDase proteins indicate that this enzyme family is highly conserved within organisms. The deduced amino acid alignment among zebrafish NTPDase sequences allowed the identification of the five apyrase conserved regions (ACRs), conserved cysteine residues, transmembrane domains, possible signal peptides, and putative regulatory sites related to posttranslational modifications (Fig. 4).

The presence of two hydrophobic domains was predicted for most zebrafish NTPDase ortholog sequences. However, NTPDase2_mg presented a single transmembrane domain at the C-terminal region. Meanwhile, analysis of zebrafish NTPDase5_ms, NTPDase6 and NTPDase8 showed the presence of one transmembrane domain at the N-terminal region, whereas the predicted NTPDase5_me sequence did not contain a characteristic hydrophobic domain at all. Several predicted cysteine residues and putative posttranslational modification sites were aligned consistently among the enzymes, suggesting a possible conservation of these amino acid residues in the zebrafish NTPDase family (Fig. 4).

3.4. Transcriptional analysis of entpd genes

Considering the presence of NTPDase activity in zebrafish tissues and the identification of distinct members of this enzyme family in this species, the relative *entpd* gene expression profile in the brain, liver, and heart was determined by RT-PCR experiments (Fig. 5). The PCR products obtained for each *entpd* primer were specific, displayed the expected fragment sizes and were identical to their respective sequences retrieved from databases. Higher amounts of *entpd1* and *entpd3* transcripts were detected in brain, with an intermediate expression level in liver, while less abundant mRNA was found in heart. Concerning the three *entpd2* paralogs, it was found that all these genes are differently expressed in zebrafish tissues. The

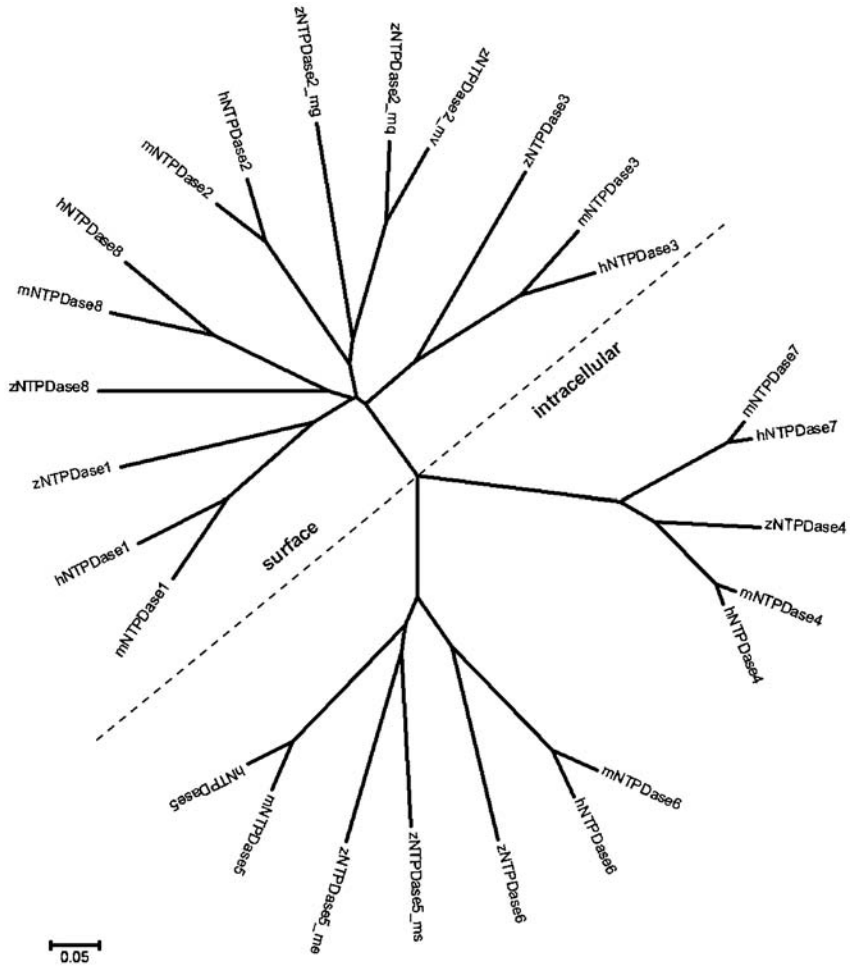

Fig. 3. Phylogenetic analysis of NTPDase family members in zebrafish (z) showing the surface-located and intracellular enzymes consistently grouped with their respective human (h) and mouse (m) orthologs. The deduced amino acid sequences were aligned with the ClustalX program and the phylogenetic tree was constructed using the Neighbor-Joining method and proportional (*p*) distance with the MEGA 4.0 program.

entpd2_mg and *entpd2_mq* genes were less expressed in liver when compared to brain, and large amounts of transcripts of *entpd2* paralogs were detected in heart. Brain and liver had similar levels of *entpd4* transcripts, whereas a lower *entpd4* expression was detected in heart. In relation to *entpd5* expression, the *entpd5_ms* was highly expressed in brain and less expressed in heart. The expression of the *entpd5_me* gene was also investigated and the results demonstrated that a similar amount of mRNA was present in brain and liver, with a lower abundance in heart. Expression of the *entpd6* gene was similar in the three tissues tested, while a lower mRNA level for *entpd8* was detected in brain when compared to liver and heart. Representative RT-PCR experiments demonstrating the *β-actin* amplification (Fig. 5A) and *entpd* expression profile of the surface-located enzymes (Fig. 5B) and intracellular NTPDase members (Fig. 5C) are shown.

4. Discussion

In the present report we describe some biochemical and molecular features of the NTPDase family in zebrafish. Although the presence of ATP and/or ADP hydrolyzing activity had been described for several decades in distinct cell types, the molecular identity of the first member of the NTPDase family (*entpd1*) remained unknown until the mid-1990 s (Robson et al., 2006). Since the structural and functional characterization of the ionotropic P2X receptor from zebrafish suggested that ATP-mediated responses were selected early in the vertebrate phylogeny (Boué-Grabot et al., 2000), several studies have shown the importance of purinergic signaling in this species (Kucenas et al., 2003; Rico et al., 2003; Senger et al., 2004; Ricatti et al., 2009). However, besides the identification and confirmation of different NTPDase sequences by a phylogenetic analysis, this is the first study to demonstrate the mRNA expression profile of all the *entpd* family members identified so far in the brain, liver, and heart of zebrafish. Thus, it appears that these tissues are able to hydrolyze both ATP and ADP in a divalent cation-dependent manner.

Here we demonstrate an easy and rapid tissue preparation useful for studying the nucleotide hydrolysis and the influence of several inhibitors on NTPDase activities in different zebrafish organs that require a small amount of protein for enzyme assays (3–5 μg). The distinct ATPase inhibitors tested did not cause any significant changes in ATP and ADP hydrolysis in zebrafish brain, liver, and heart. Therefore, a possible contamination with classical ATPases in our fraction did not significantly influence nucleotide hydrolysis in the tissues analyzed. Moreover, Ca^{2+}-ATP was chosen as the substrate in this study because it can also eliminate interference by P-type ATPases, which are not activated by Ca^{2+} alone. Sodium azide is a well-known inhibitor of the mitochondrial ATPase, acting on both F_oF_1 and soluble F_1, indicating that the inhibitory site for azide is on F_1, with an I_{50} of 0.04 mM (Pullman et al., 1960). However, it has been reported that high concentrations of this compound are able to inhibit ATP diphosphohydrolase activity from several sources, including the ATP and ADP hydrolysis in zebrafish brain membranes (Plesner, 1995; Rico et al., 2003; Rücker et al., 2008). In our experiments, 20 mM sodium azide significantly decreased both ATP and ADP hydrolysis in the brain, liver, and heart. Meanwhile, ARL 67156 and Suramin, two

Table 4
Relatedness between the *Danio rerio* (Dr) NTPDase (D) proteins and their *Homo sapiens* (Hs) and *Mus musculus* (Mm) orthologs.

A

	DrD1	HsD1	MmD1	DrD2_mg	DrD2_mq	DrD2_mv	HsD2	MmD2	DrD3	HsD3	MmD3	DrD8	HsD8	MmD8
DrD1	·····	51.8	51.4	38.4	42.2	42.5	42.1	42.4	39.1	41.0	38.9	43.1	40.5	40.7
HsD1	68.8	·····	75.8	37.0	40.5	40.8	38.6	41.0	38.5	36.7	36.4	39.7	42.6	43.2
MmD1	67.6	86.5	·····	38.1	41.1	40.5	39.5	42.0	39.0	37.7	36.8	39.8	39.7	41.9
DrD2_mg	57.9	58.3	58.1	·····	50.7	51.4	45.7	47.0	35.2	38.4	35.8	38.7	34.8	36.2
DrD2_mq	61.0	61.6	61.2	69.1	·····	75.2	49.0	49.4	37.2	38.9	36.7	40.1	39.5	39.1
DrD2_mv	60.0	59.8	58.8	73.0	83.1	·····	48.4	48.9	37.2	37.6	37.6	41.5	37.9	38.5
HsD2	58.6	57.5	58.6	63.0	67.4	66.5	·····	83.4	34.4	38.5	39.3	42.9	42.7	42.2
MmD2	60.0	60.2	60.4	65.0	67.8	68.7	90.3	·····	35.0	38.5	39.7	43.3	43.3	43.4
DrD3	58.1	59.5	58.9	57.7	59.1	58.5	55.8	57.3	·····	48.8	45.1	37.8	35.1	35.6
HsD3	57.7	56.5	56.3	57.7	57.8	56.9	56.0	58.4	65.8	·····	81.1	37.6	38.4	37.9
MmD3	57.3	53.9	55.0	54.8	56.9	58.0	56.9	58.4	64.5	89.6	·····	37.9	38.2	38.5
DrD8	61.6	58.4	59.2	57.9	61.6	59.8	60.6	62.8	56.9	54.3	53.9	·····	44.2	45.6
HsD8	58.4	61.0	57.5	55.4	59.4	57.8	60.8	59.0	53.9	55.0	55.8	61.4	·····	74.1
MmD8	59.8	61.6	60.2	56.4	60.8	59.2	60.6	60.8	56.9	54.6	56.9	62.4	85.9	·····

B

	DrD4	HsD4	MmD4	DrD5_ms	DrD5_me	HsD5	MmD5	DrD6	HsD6	MmD6
DrD4	·····	64.8	70.1	20.1	18.8	20.2	20.6	20.1	21.0	21.2
HsD4	77.3	·····	83.0	22.0	19.7	21.2	20.5	22.4	22.1	22.6
MmD4	84.3	88.3	·····	21.5	19.2	20.6	19.9	21.0	21.4	22.7
DrD5_ms	36.0	38.4	34.7	·····	48.0	52.2	51.1	43.6	42.7	45.7
DrD5_me	37.5	38.7	36.2	63.5	·····	43.4	42.8	36.2	37.6	38.1
HsD5	34.2	36.8	33.9	68.5	56.6	·····	88.1	43.4	44.7	46.8
MmD5	34.7	36.6	33.8	67.7	55.9	93.7	·····	43.7	44.5	47.4
DrD6	32.7	36.4	34.6	60.3	51.4	60.4	59.5	·····	49.6	52.1
HsD6	35.5	37.7	35.1	60.5	55.5	57.8	58.8	62.7	·····	82.6
MmD6	35.4	37.7	35.7	62.9	53.4	59.1	61.3	66.4	87.8	·····

Note: The percentage of amino acid identity (black boxes) and similarity (gray boxes) between the proteins was determined by the scoring matrix BLOSUM62 using MatGAT 2.01 software.
A — Comparison between surface-located NTPDase members.
B — Comparison between intracellular NTPDase members.

ATPDase inhibitors, differentially altered the nucleotide hydrolysis assayed. In comparison to ARL 67156, Suramin was a more potent inhibitor of nucleotide hydrolysis in zebrafish tissues even though ARL 67156 had a partial, but significant inhibitory effect on ADP hydrolysis in brain. It has been recently reported that ARL 67156 is a weak competitive inhibitor of human NTPDase1 and NTPDase3, and partially inhibits the mouse and human forms of these enzymes in the micromolar range, being less effective against NTPDase2 and NTPDase8 (Lévesque et al., 2007). In another work Suramin was also observed to strongly inhibit both ecto-ATPase and -ADPase hydrolytic activities in recombinant *Trypanosoma cruzi* NTPDase-1 and in live trypomastigotes (Santos et al., 2009) at the same concentrations tested in our study. We cannot exclude the possibility that the inhibitors used here had an additional action on other molecular targets such as P2 receptors, which have been shown to be susceptible to blockade by Suramin (von Kügelgen, 2006), or even that the high substrate concentrations used in the enzyme assays might have partially overcome the blockade effected by ARL 67156. Although more selective NTPDase inhibitors, such as sodium polyoxotungstate (Wall et al., 2008) were not used in this study, our results suggest that the distinct profile of ATP and ADP hydrolysis observed in the range of time and protein concentration could be attributed to the existence of different NTPDase members cleaving tri- and diphosphonucleosides in brain, liver, and heart of zebrafish.

Ten zebrafish NTPDase orthologs (NTPDase1–6 and 8) were found to be present by phylogenetic analysis. A previous study from our laboratory had already identified the presence of three independent *entpd2* genes in zebrafish (*entpd2_mg*, *entpd2_mq*, and *entpd2_mv*) (Rico et al., 2006); however, here, for the first time, two distinct *entpd5* (*entpd5_ms* and *entpd5_me*), *entpd6*, and *entpd8* sequences were also identified in the zebrafish genome. It is tempting to speculate that the presence of three NTPDase2 and two NTPDase5 paralog proteins in zebrafish could be a consequence of genome-wide duplication in the teleost radiation, which has been previously reported in the literature (Amores et al., 1998). In fact, several studies have demonstrated the existence of duplicated genes in zebrafish (Amores et al., 1998; Rosemberg et al., 2007). Concerning purinergic signaling, it has been recently reported that the zebrafish family of ionotropic P2X receptors is comprised of nine members with two paralog copies of $P2X_3$, $P2X_4$, and $P2X_5$ (Low et al., 2008). The NTPDase7 ortholog was not detected in zebrafish, which lead us to hypothesize that its respective gene might not yet have been characterized or even that this member might have been lost from the zebrafish genome during evolution. Interestingly, Low et al. (2008) did not find a gene encoding $P2X_6$ in the zebrafish genome, which shows that nucleotide-mediated signaling in this teleost could differ from mammals and be more complex than previously thought. The identification of three NTPDase2 and two NTPDase5 paralogs in zebrafish suggests that they might be important for a differential regulation of nucleotide signaling in this species.

The phylogeny also showed that zebrafish NTPDase4, NTPDases5 and 6 are separated into two different subfamilies. This separation is probably due to their biochemical properties, which may be similar to the intracellular NTPDase members previously characterized in mammals (Robson et al., 2006). Using bioinformatics tools we verified that zebrafish NTPDase4 presents two transmembrane domains, whereas different hydrophobic domain numbers were identified for NTPDase5 paralogs and NTPDase6. Moreover, sequence analysis of NTPDase2_mg and NTPDase8 showed the presence of a single transmembrane domain for both proteins. Considering that transmembrane domain interactions can modify the stability of the extracellular portion of the human NTPDase2 (Chiang and Knowles, 2008), the difference in the number of hydrophobic domains observed among zebrafish NTPDase sequences might contribute to a distinct

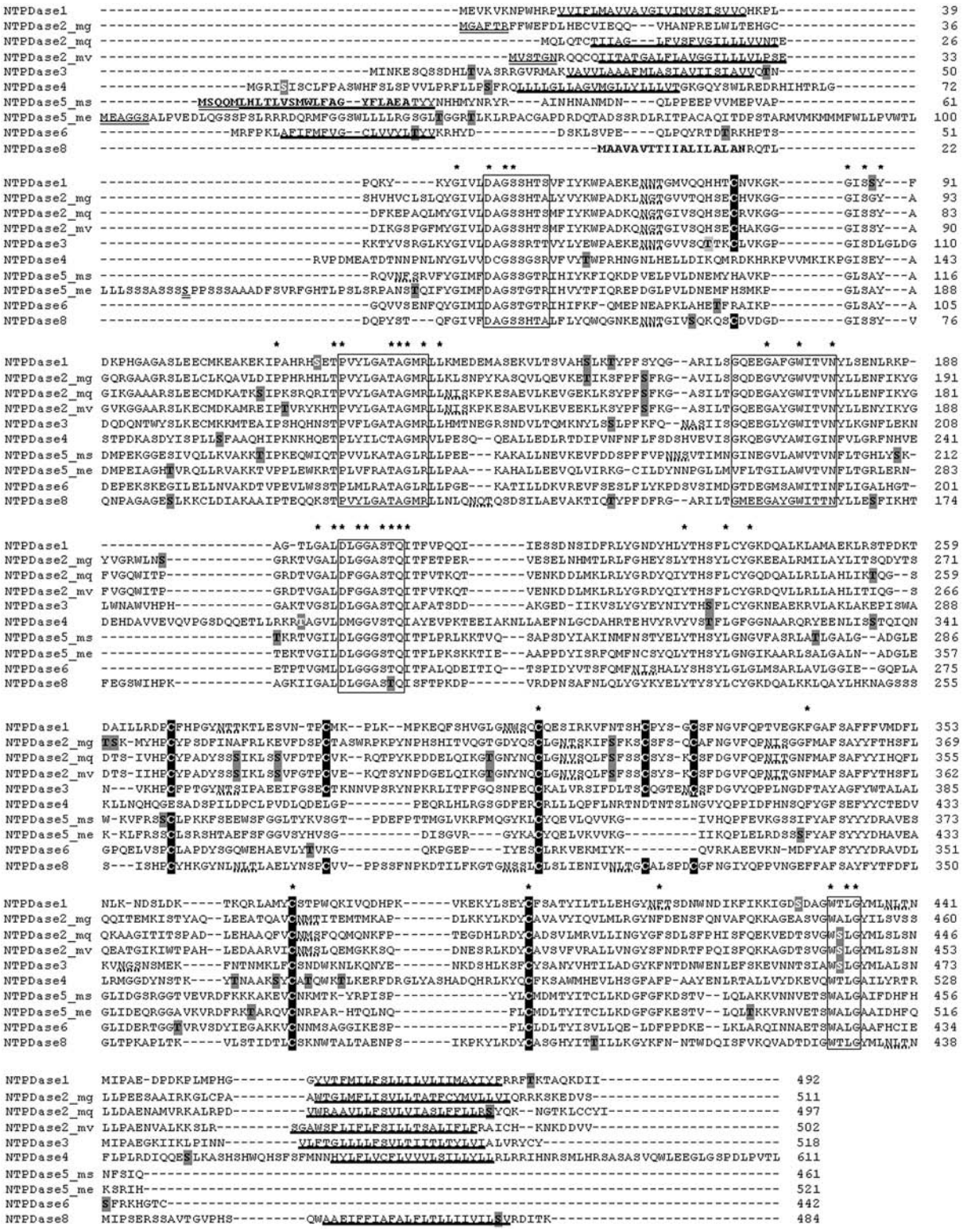

Fig. 4. Alignment of deduced amino acid sequences for the zebrafish NTPDase family members. The conserved apyrase domains (ACRs) are represented in the boxes. The transmembrane domains are underlined and the signal peptide from NTPDase5_ms is in bold face. Potential *N*-glycosylation and N-acetylation sites are shown by dotted lines and double underline, respectively. Conserved cysteine residues are bold face in black boxes. Putative PKA and PKC phosphorylation sites are marked in gray boxes with white and black letters, respectively. The asterisks (*) indicate similarities among all zebrafish NTPDase members after ClustalX alignment.

anchorage stability and enzyme activity. Although further studies are still required to clarify the involvement of hydrophobic domains in zebrafish NTPDase activities it is possible to speculate that NTPDase5_me might act as a soluble enzyme or even possess another membrane anchorage mechanism since its sequence did not present a characteristic transmembrane domain.

Posttranslational processes are responsible for regulating several enzyme activities and modulate metabolic pathways. Although there

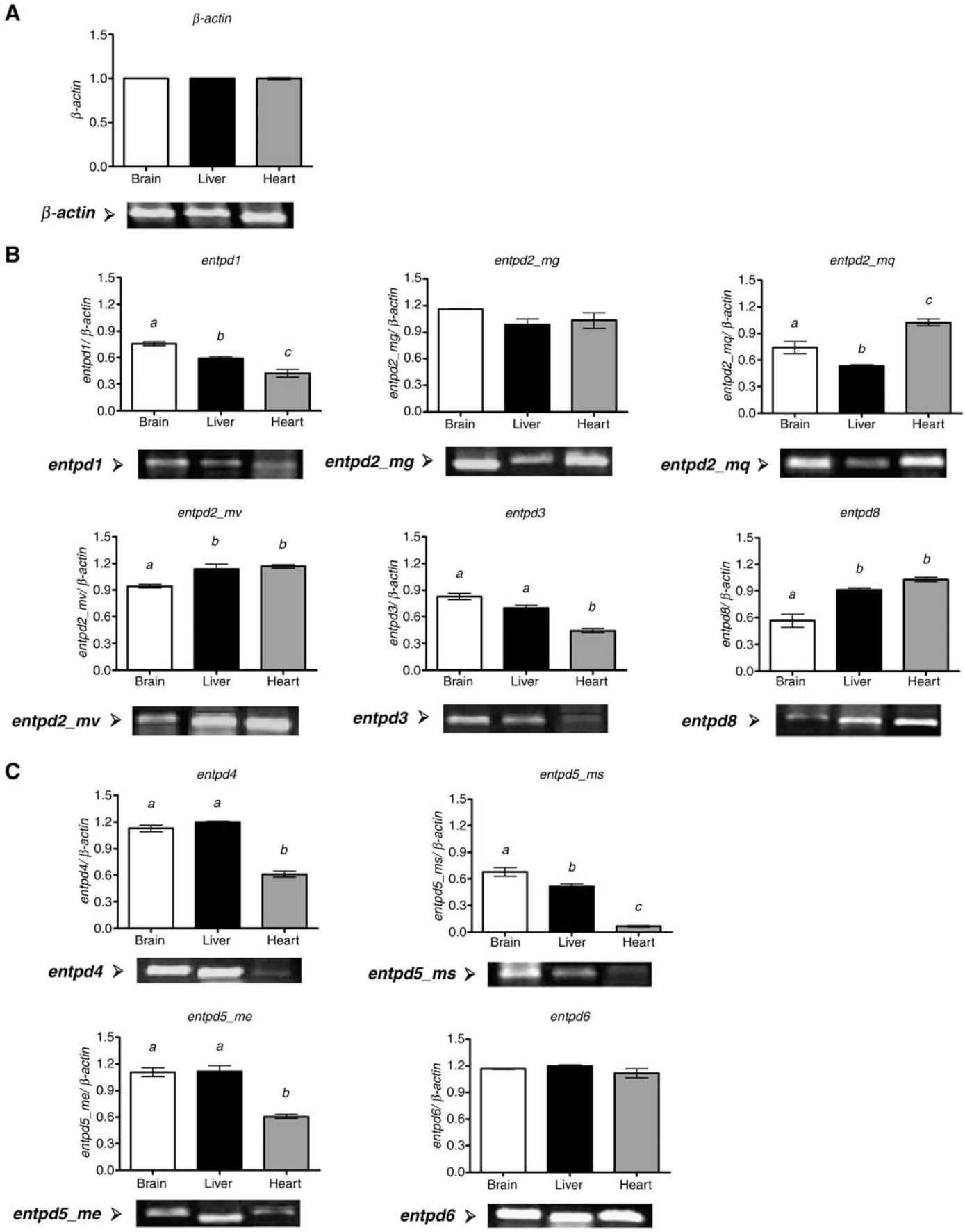
A
β-actin
β-actin
Brain
Liver
Heart
β-actin
B
entpd1
entpd2_mg
entpd2_mq
entpd2_mv
entpd3
entpd8
C
entpd4
entpd5_ms
entpd5_me
entpd6

are no experimental data for phosphorylation mechanisms on ectonucleotidases so far, PKC target residues for zebrafish NTPDase members were also aligned with other putative PKC regulatory sites on mammalian orthologs, such as human Lys62 and Asn64 from the NTPDase2 sequence (data not shown). Given that both regions have been described as essential structural elements for the enzyme (Javed et al., 2007) the conservation of these phosphorylation sites could indicate that PKC activity may be important for the mediation of posttranslational events in vertebrate NTPDase members. In the same way, a previous study reported that N-termini of NTPDases also contain consensus sequences for protein phosphorylation by PKC (Kegel et al., 1997).

Here we also verified that conserved asparagine residues from zebrafish NTPDase1, NTPDase2_mg, NTPDase2_mq, NTPDase2_mv, NTPDase3, and NTPDase8 (Asn69, Asn71, Asn61, Asn68, Asn85, and Asn 54, respectively) were predicted as putative *N*-glycosylation sites. A recent study showing asparagine-to-glutamine mutation at six individual potential *N*-linked glycosylation sites from human NTPDase2 established the importance for protein function and expression of Asn64, which is conserved in all cell surface NTPDases (Javed et al., 2007). The proximity of these respective residues with Asn64 from human NTPDase2 obtained by alignment of the sequences (data not shown), associated with the separation of NTPDase1-3 and 8 from NTPDase4-6 clades corroborated by our phylogenetic analysis, strongly supports the idea that these members act as ecto-enzymes in zebrafish.

The RT-PCR assays in the present study showed a distinct expression profile for the three *entpd2* paralogs (*entpd2_mg*, *mq*, and *mv*) in zebrafish brain, as previously reported (Rico et al., 2006, 2008). Despite the lower *entpd5_ms* expression in heart, large amounts of *entpd2* paralogs and *entpd6* transcripts could be detected in this tissue. These data are in accordance with the literature, since NTPDase activity in rat left ventricle is associated with a high *entpd2* expression and NTPDase6 may participate in homeostasis by playing a role in ADP hydrolysis in heart (Yeung et al., 2000; Rücker et al., 2008). Interestingly, in contrast to mammals, *entpd8* transcripts were detected in zebrafish brain, even though at lower levels than in the liver and heart. The high *entpd8* expression level detected in liver could indicate a possible relevance of this enzyme to the hepatic physiology of zebrafish since the main hepatic ecto-ATPDase activity in mammals has been attributed to the canalicular *entpd8* expression, which is involved in the regulation of bile secretion and/or nucleoside salvage (Fausther et al., 2007). In addition, the differential *entpd1*, *entpd2*, and *entpd3* expression observed in zebrafish liver could be important for the regulation of several metabolic pathways since there is evidence that extracellular nucleotides play a role in the control of glycogenolysis and in the activation of JNK signaling (Keppens et al., 1989; Thevananther et al., 2004; Robson et al., 2006). Furthermore, the presence of at least two members of the surface-located NTPDase family has been observed in intact goldfish hepatocytes, suggesting that distinct enzymes may account for the hydrolysis of extracellular nucleotides in the liver of this teleost (Alleva et al., 2002).

Despite the identification of ten distinct *entpd* transcripts, the possibility remains that splice variants exist for the NTPDase members, since transcript variants from NTPDases have already been demonstrated in different organisms (Vlajkovic et al., 1999; Biederbick et al., 2000; Mateo et al., 2003). Thus, the involvement of possible NTPDase isoforms in nucleotide hydrolysis in zebrafish tissues still requires further investigation.

In conclusion, our findings demonstrate that several NTPDase members may hydrolyze tri- and diphosphonucleosides in zebrafish tissues. Our data reinforce the idea that zebrafish represent a useful vertebrate model for studying distinct purinergic signaling parameters. The elucidation of zebrafish NTPDase members should certainly contribute to better understanding of this enzyme family in this species.

Acknowledgements

This work was supported by Coordenação de Aperfeiçoamento de Pessoal de Nível Superior (CAPES), Conselho Nacional de Desenvolvimento Científico e Tecnológico (CNPq), Fundação de Amparo à Pesquisa do Estado do Rio Grande do Sul (FAPERGS) and by the FINEP research grant "Rede Instituto Brasileiro de Neurociência (IBN-Net)" #01.06.0842-00. D.B.R was a recipient of a fellowship from CAPES; E.P.R and A.S.L were recipients of fellowships from CNPq; J.T.S. was a recipient of a fellowship from FAPERGS. The authors would like to thank to Dr. Gareth Cuttle for the English correction and editing of the manuscript.

References

Alleva, K.E., Espelt, M.V., Krumschnabel, G., Schwarzbaum, P.J., 2002. Identification of two distinct E-NTPDases in liver of goldfish (*Carassius auratus* L.). Comp. Biochem. Physiol. B Biochem. Mol. Biol. 131, 725–731.

Amores, A., Force, A., Yan, Y.L., Joly, L., Amemiya, C., Fritz, A., Ho, R.K., Langeland, J., Prince, V., Wang, Y.L., Westerfield, M., Ekker, M., Postlethwait, J.H., 1998. Zebrafish hox clusters and vertebrate genome evolution. Science 282, 1711–1714.

Appelbaum, L., Skariah, G., Mourrain, P., Mignot, E., 2007. Comparative expression of P2X receptors and ecto-nucleoside triphosphate diphosphohydrolase 3 in hypocretin and sensory neurons in zebrafish. Brain Res. 1174, 66–75.

Baraban, S.C., 2007. Emerging epilepsy models: insights from mice, flies, worms and fish. Curr. Opin. Neurol. 20, 164–168.

Barnes, J.M., Murphy, P.A., Kirkham, D., Henley, J.M., 1993. Interaction of guanine nucleotides with [3H]kainate and 6-[3H]cyano-7-nitroquinoxaline-2, 3-dione binding in goldfish brain. J. Neurochem. 61, 1685–1691.

Barreto-Chaves, M.L., Carneiro-Ramos, M.S., Cotomacci, G., Júnior, M.B., Sarkis, J.J., 2006. E-NTPDase 3 (ATP diphosphohydrolase) from cardiomyocytes, activity and expression are modulated by thyroid hormone. Mol. Cell. Endocrinol. 251, 49–55.

Beldi, G., Wu, Y., Sun, X., Imai, M., Enjyoji, K., Csizmadia, E., Candinas, D., Erb, L., Robson, S.C., 2008. Regulated catalysis of extracellular nucleotides by vascular CD39/ENTPD1 is required for liver regeneration. Gastroenterology 135, 1751–1760.

Biederbick, A., Kosan, C., Kunz, J., Elsässer, H.P., 2000. First apyrase splice variants have different enzymatic properties. J. Biol. Chem. 275, 19018–19024.

Bonan, C.D., Dias, M.M., Battastini, A.M., Dias, R.D., Sarkis, J.J., 1998. Inhibitory avoidance learning inhibits ectonucleotidases activities in hippocampal synaptosomes of adult rats. Neurochem. Res. 23, 977–982.

Bonan, C.D., Amaral, O.B., Rockenbach, I.C., Walz, R., Battastini, A.M., Izquierdo, I., Sarkis, J.J., 2000. Altered ATP hydrolysis induced by pentylenetetrazol kindling in rat brain synaptosomes. Neurochem. Res. 25, 775–779.

Boué-Grabot, E., Akimenko, M.A., Séguéla, P., 2000. Unique functional properties of a sensory neuronal P2X ATP-gated channel from zebrafish. J. Neurochem. 75, 1600–1607.

Bradford, M.M., 1976. A rapid and sensitive method for the quantification of microgram quantities of protein utilizing the principle of protein-dye binding. Anal. Biochem. 72, 218–254.

Burnstock, G., 2009. Purinergic cotransmission. Exp. Physiol. 94, 20–24.

Campanella, J.J., Bitincka, L., Smalley, J., 2003. MatGAT: an application that generates similarity/identity matrices using protein or DNA sequences. BMC Bioinformatics 4, 29.

Chan, K.M., Delfert, D., Junger, K.D., 1986. A direct colorimetric assay for Ca^{2+}-stimulated ATPase activity. Anal. Biochem. 157, 375–380.

Chen, W.-Y., John, J.A.C., Lin, C.-H., Lin, H.-F., Wu, S.-C., Lin, C.-H., Chang, C.-Y., 2004. Expression of metallothionen gene during embryonic and early larval development in zebrafish. Aquat. Toxicol. 69, 215–227.

Chiang, W.C., Knowles, A.F., 2008. Transmembrane domain interactions affect the stability of the extracellular domain of the human NTPDase 2. Arch. Biochem. Biophys. 472, 89–99.

Chico, T.J., Ingham, P.W., Crossman, D.C., 2008. Modeling cardiovascular disease in the zebrafish. Trends Cardiovasc. Med. 18, 150–155.

Fausther, M., Lecka, J., Kukulski, F., Lévesque, S.A., Pelletier, J., Zimmermann, H., Dranoff, J.A., Sévigny, J., 2007. Cloning, purification, and identification of the liver canalicular

Fig. 5. Relative expression profiles of the *entpd* genes in different adult zebrafish tissues. The figure shows representative RT-PCR experiments and the optical densitometry analysis for *β-actin* (A) and *entpd* members (surface-located enzymes (B) and intracellular NTPDases (C)). Four independent experiments were performed, with entirely consistent results (ANOVA, followed by Tukey HSD test as post-hoc, $P \leq 0.05$).

ecto-ATPase as NTPDase8. Am. J. Physiol. Gastrointest. Liver Physiol. 292, G785–G795.
Javed, R., Yarimizu, K., Pelletier, N., Li, C., Knowles, A.F., 2007. Mutagenesis of lysine 62, asparagine 64, and conserved region 1 reduces the activity of human ecto-ATPase (NTPDase 2). Biochemistry 46, 6617–6627.
Kegel, B., Braun, N., Heine, P., Maliszewski, C.R., Zimmermann, H., 1997. An ecto-ATPase and an ecto-ATP diphosphohydrolase are expressed in rat brain. Neuropharmacology 36, 1189–1200.
Keppens, S., VandeKerckhove, J., Wulf, H.De., 1989. Characterization of purinoceptors present on human liver plasma membranes. FEBS Lett. 248, 137–140.
Kirley, T.L., Crawford, P.A., Smith, T.M., 2006. The structure of the nucleoside triphosphate diphosphohydrolases (NTPDases) as revealed by mutagenic and computational modeling analyses. Purinergic Signal. 2, 379–389.
Köhler, D., Eckle, T., Faigle, M., Grenz, A., Mittelbronn, M., Laucher, S., Hart, M.L., Robson, S.C., Müller, C.E., Eltzschig, H.K., 2007. CD39/ectonucleoside triphosphate diphosphohydrolase 1 provides myocardial protection during cardiac ischemia/reperfusion injury. Circulation 116, 1784–1794.
Kucenas, S., Li, Z., Cox, J.A., Egan, T.M., Voigt, M.M., 2003. Molecular characterization of the zebrafish P2X receptor subunit gene family. Neuroscience 121, 935–945.
Lavoie, E.G., Kukulski, F., Lévesque, S.A., Lecka, J., Sévigny, J., 2004. Cloning and characterization of mouse nucleoside triphosphate diphosphohydrolase-3. Biochem. Pharmacol. 67, 1917–1926.
Lévesque, S.A., Lavoie, E.G., Lecka, J., Bigonnesse, F., Sévigny, J., 2007. Specificity of the ecto-ATPase inhibitor ARL 67156 on human and mouse ectonucleotidases. Br. J. Pharmacol. 152, 141–150.
Low, S.E., Kuwanda, J.Y., Hume, R.I., 2008. Amino acid variations resulting in functional and nonfunctional zebrafish $P2X_1$ and $P2X_{5.1}$ receptors. Purinergic Signal 4, 383–392.
Mateo, J., Kreda, S., Henry, C.E., Harden, T.K., Boyer, J.L., 2003. Requirement of Cys399 for processing of the human ecto-ATPase (NTPDase2) and its implications for determination of the activities of splice variants of the enzyme. J. Biol. Chem. 278, 39960–39968.
Murphy-Piedmonte, D.M., Crawford, P.A., Kirley, T.L., 2005. Bacterial expression, folding, purification and characterization of soluble NTPDase5 (CD39L4) ecto-nucleotidase. Biochim. Biophys. Acta 1747 (2), 251–259.
Plesner, L., 1995. Ecto-ATPases: identities and functions. Int. Rev. Cytol. 158, 141–214.
Pullman, M.E., Penefsky, H.S., Datta, A., Racker, E., 1960. Partial resolution of the enzymes catalyzing oxidative phosphorylation. I. Purification and properties of soluble dinitrophenol-stimulated adenosine triphosphatase. J. Biol. Chem. 235, 3322–3329.
Rekha, R.D., Amali, A.A., Her, G.M., Yeh, Y.H., Gong, H.Y., Hu, S.Y., Lin, G.H., Wu, J.L., 2008. Thioacetamide accelerates steatohepatitis, cirrhosis and HCC by expressing HCV core protein in transgenic zebrafish *Danio rerio*. Toxicology 243, 11–22.
Ricatti, M.J., Alfie, L.D., Lavoie, E.G., Sévigny, J., Schwarzbaum, P.J., Faillace, M.P., 2009. Immunocytochemical localization of NTPDases1 and 2 in the neural retina of mouse and zebrafish. Synapse 63 (4), 291–307.
Rico, E.P., Senger, M.R., Fauth, Mda.G., Dias, R.D., Bogo, M.R., Bonan, C.D., 2003. ATP and ADP hydrolysis in brain membranes of zebrafish (*Danio rerio*). Life Sci. 73, 2071–2082.
Rico, E.P., Rosemberg, D.B., Senger, M.R., Arizi, Mde.B., Bernardi, G.F., Dias, R.D., Bogo, M.R., Bonan, C.D., 2006. Methanol alters ecto-nucleotidases and acetylcholinesterase in zebrafish brain. Neurotoxicol. Teratol. 28, 489–496.
Rico, E.P., Rosemberg, D.B., Senger, M.R., Arizi, M., de Bem Dias, R.D., Souto, A.A., Bogo, M.R., Bonan, C.D., 2008. Ethanol and acetaldehyde alter NTPDase and 5′-nucleotidase from zebrafish brain membranes. Neurochem. Int. 52, 290–296.
Robson, S.C., Sévigny, J., Zimmermann, H., 2006. The E-NTPDase family of ectonucleotidases: structure function relationships and pathophysiological significance. Purinergic Signal 2, 409–430.
Rosemberg, D.B., Rico, E.P., Guidoti, M.R., Dias, R.D., Souza, D.O., Bonan, C.D., Bogo, M.R., 2007. Adenosine deaminase-related genes: molecular identification, tissue expression pattern and truncated alternative splice isoform in adult zebrafish (*Danio rerio*). Life Sci. 81, 1526–1534.
Rücker, B., Almeida, M.E., Libermann, T.A., Zerbini, L.F., Wink, M.R., Sarkis, J.J., 2008. E-NTPDases and ecto-5′-nucleotidase expression profile in rat heart left ventricle and the extracellular nucleotide hydrolysis by their nerve terminal endings. Life Sci. 82, 477–486.
Saitou, N., Nei, M., 1987. The neighbor-joining method: a new method for reconstructing phylogenetic trees. Mol. Biol. Evol. 4, 406–425.
Santos, R.F., Pôssa, M.A., Bastos, M.S., Guedes, P.M., Almeida, M.R., Demarco, R., Verjovski-Almeida, S., Bahia, M.T., Fietto, J.L., 2009. Influence of ecto-nucleoside triphosphate diphosphohydrolase activity on *Trypanosoma cruzi* infectivity and virulence. PLoS Negl. Trop. Dis. 3 (3), e387.
Schetinger, M.R., Morsch, V.M., Bonan, C.D., Wyse, A.T., 2007. NTPDase and 5′-nucleotidase activities in physiological and disease conditions: new perspectives for human health. Biofactors 31, 77–98.
Senger, M.R., Rico, E.P., Dias, R.D., Bogo, M.R., Bonan, C.D., 2004. Ecto-5′-nucleotidase activity in brain membranes of zebrafish (*Danio rerio*). Comp. Biochem. Physiol. B Biochem. Mol. Biol. 139, 203–207.
Tamura, K., Dudley, J., Nei, M., Kumar, S., 2007. MEGA4: molecular evolutionary genetics analysis (MEGA) software version 4.0. Mol. Biol. Evol. 24, 1596–1599.
Thevananther, S., Sun, H., Li, D., Arjunan, V., Awad, S.S., Wyllie, S., Zimmerman, T.L., Goss, J.A., Karpen, S.J., 2004. Extracellular ATP activates c-Jun N-terminal kinase signalling and cell cycle progression in hepatocytes. Hepatology 39, 393–402.
Thompson, J.D., Gibson, T.J., Plewniak, F., Jeanmougin, F., Higgins, D.G., 1997. The CLUSTAL_X windows interface: flexible strategies for multiple sequence alignment aided by quality analysis tools. Nucleic Acids Res. 25, 4876–4882.
Vlajkovic, S.M., Housley, G.D., Greenwood, D., Thorne, P.R., 1999. Evidence for alternative splicing of ecto-ATPase associated with termination of purinergic transmission. Brain Res. Mol. Brain Res. 73, 85–92.
von Kügelgen, I., 2006. Pharmacological profiles of cloned mammalian P2Y-receptor subtypes. Pharmacol. Ther. 110, 415–432.
Wall, M.J., Wigmore, G., Lopatár, J., Frenguelli, B.G., Dale, N., 2008. The novel NTPDase inhibitor sodium polyoxotungstate (POM-1) inhibits ATP breakdown but also blocks central synaptic transmission, an action independent of NTPDase inhibition. Neuropharmacology 55, 1251–1258.
Yeung, G., Mulero, J.J., McGowan, D.W., Bajwa, S.S., Ford, J.E., 2000. CD39L2, a gene encoding a human nucleoside diphosphatase, predominantly expressed in the heart. Biochemistry 39, 12916–12923.
Zimmermann, H., 2001. Ectonucleotidases: some recent developments and a note on nomenclature. Drug Dev. Res. 52, 44–56.
Zimmermann, H., 2006. Ectonucleotidases in the nervous system. Novartis Found. Symp. 276, 113–128 discussion 128–130, 233–237, 275–281.